Volume 58
Number 53
7 July 2022
Pages 7327–7440

ChemComm

Chemical Communications

rsc.li/chemcomm

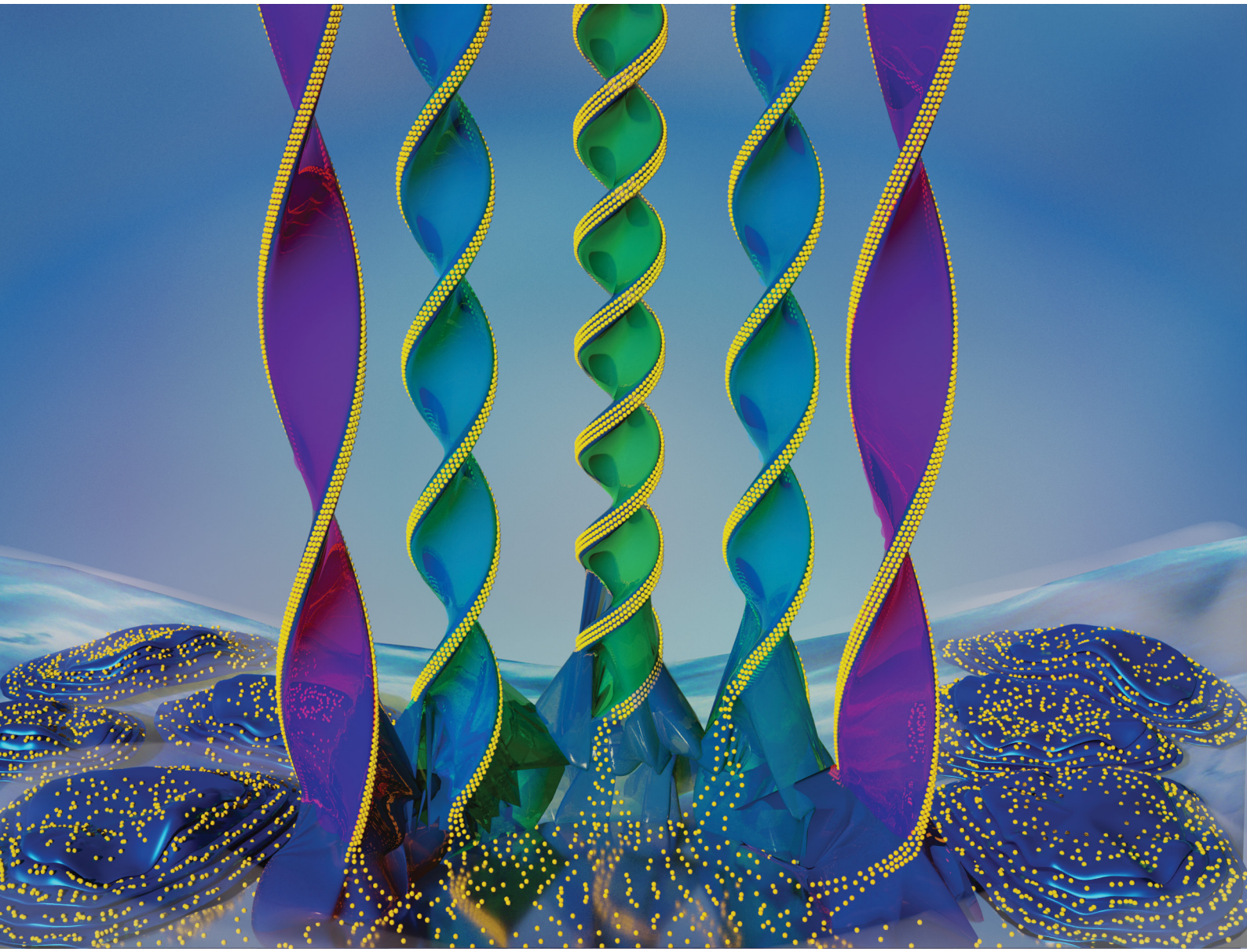

ISSN 1359-7345

ROYAL SOCIETY OF CHEMISTRY

COMMUNICATION

Wiktor Lewandowski *et al.*

Tuneable helices of plasmonic nanoparticles using liquid crystal templates: molecular dynamics investigation of an unusual odd–even effect in liquid crystalline dimers

ChemComm

COMMUNICATION

View Article Online
View Journal | View Issue

Cite this: *Chem. Commun.*, 2022, **58**, 7364

Received 16th February 2022,
Accepted 29th April 2022

DOI: 10.1039/d2cc00560c

rsc.li/chemcomm

Tuneable helices of plasmonic nanoparticles using liquid crystal templates: molecular dynamics investigation of an unusual odd–even effect in liquid crystalline dimers†

Mateusz Pawlak,[a] Maciej Bagiński,[a] Pablo Llombart,[b] Dominik Beutel,[c] Guillermo González-Rubio,[d] Ewa Górecka,[e] Carsten Rockstuhl,[cf] Józef Mieczkowski,[a] Damian Pociecha[e] and Wiktor Lewandowski*[a]

Liquid crystalline (LC) dimers formed helical nanofilaments depending on the parity of the alkyl linker, revealing an unusual odd–even effect. Molecular dynamics simulations were used to investigate the observed tendency. Elongation of the linker translates to an increase of the pitch of the helices, which allows achieving tuneable helical assemblies of Au nanoparticles doped to the LC matrix. The impact of the tuneable pitch of helices on the chiral optical properties of composites was investigated with full-wave simulations based on the T-matrix method.

Thin films of gold nanoparticles (NPs) exhibiting plasmonic circular dichroism (PCD)[1] are foreseen to revolutionise photonic technologies of the 21st century.[2] Unfortunately, the availability of thin film materials exhibiting PCD properties is highly limited. A common way to fabricate materials exhibiting chiral structures (and thus properties) is the use of organic molecules that can act as small building blocks organising into 3D mesoscopic objects. When doped with gold NPs, these objects can serve as templates for their organisation, thereby inducing PCD properties. Although research exploiting this powerful approach is dynamically progressing for aqueous dispersions, translating these achievements to the realm of thin films is challenging. The foremost limiting step is the precise control over the helical morphology of the templates in the form of thin film, which requires further progress in materials chemistry and molecular components design. One of the most perspective types of materials, which can spontaneously form chiral structures, also in thin films, are liquid crystals.[3] Chiral LCs exhibit strong chiro-optical properties and can be utilised as matrices to prepare composites in which a helical arrangement of gold NPs leads to enhanced PCD responses.[4] Interestingly, helical structures of LC phases may also be formed by achiral molecules, *e.g.* bent-core or bent dimeric molecules, limiting the requirement to introduce chirality at the molecular level, which complicates organic synthesis.[5] Such achiral molecules were recently shown to assemble into twist-bend nematic phase,[6,7] its lamellar analogue twist-bend smectic C phase,[8,9] and helical nanofilament (HNF) phases or dark conglomerate phases.[10] The HNF phase is particularly attractive for fabricating composites with gold NPs for photonic applications. Such composites can benefit from the synergy of the LC matrix soft character of the LC matrix and the strong optical properties of gold NPs.[11]

One of the challenges of designing chiral LC matrices built from achiral dimer-type mesogens is that minute changes in their molecular architecture might translate to drastic modifications of the phase sequence. For instance, a crucial parameter determining chiral phase formation is the length/parity of the linker unit in dimeric molecules. Typically, helical structures are formed by dimers with an odd number of atoms in the linker. Interestingly, in one of our recent works, we showed a mesogen that disobeys this general rule. We have reported the formation of helical nanofilaments by a dimeric compound with an even-numbered alkyl internal spacer and hydroquinone *p*-oleyloxybenzoate (HOB) arms.[11] Upon cooling from an isotropic melt, LC dimer formed an HNF phase, which could host gold NPs.[11]

Here, we investigated whether other members of the homologues series, referred to as HOB-*n*-HOB where n denotes the number of carbon atoms in the linkage, can also form twisted layered structures. Through the use of X-ray diffraction (XRD), polarised light microscopy (POM), and transmission electron microscopy (TEM), we determined phase sequences of the novel compounds, while molecular dynamic simulations were utilised to provide insights into the observed results. We also confirmed that even members of the family could be successfully used as matrices to prepare helical

[a] *Faculty of Chemistry, University of Warsaw, Ludwika Pasteura 1, 02-093 Warsaw, Poland. E-mail: wlewandowski@chem.uw.edu.pl*
[b] *Departamento de Física Teórica de la Materia Condensada, Instituto Nicolás Cabrera, Universidad Autónoma de Madrid, Madrid, Spain*
[c] *Institute of Theoretical Solid State Physics, Karlsruhe Institute of Technology, 76131 Karlsruhe, Germany*
[d] *Physical Chemistry Department of Chemistry, University of Konstanz, Universitätsstraße 10, Box 714, 78457 Konstanz, Germany*
[e] *Faculty of Chemistry, University of Warsaw, Zwirki i Wigury 101, Warsaw 02-089, Poland*
[f] *Institute of Nanotechnology, Karlsruhe Institute of Technology, 76021 Karlsruhe, Germany*

† Electronic supplementary information (ESI) available: Experimental details and supporting data. See DOI: https://doi.org/10.1039/d2cc00560c

composites with gold NPs in the thin film form. As proved by TEM imaging, structural parameters of the double-helical assemblies of gold NPs may be controlled by the length of the spacer in dimer-type mesogens. This may lead to a tuneable CD responses, as revealed by computational simulations based on the T-matrix method using double helices made of NPs.

The synthesis of a series of HOB-*n*-HOB dimers (see Fig. S1, ESI†) was conducted using a previously published protocol.[11] Shortly, the procedure started with the synthesis of the dimer arms (HOB). Two-aromatic ring arms were connected to form dimers (*via* a Mitsunobu reaction) with dialcohols having a different number of carbon atoms (*n*). Thereby, we obtained 7 novel homologues of the HOB-*n*-HOB series with n = 6–11 and 16, in addition to the previously studied HOB-12-HOB. We initially confirmed the tendency of odd and even HOB-*n*-HOB members to form layered and twisted-layered structures, respectively, using TEM imaging of heat-annealed samples (Fig. 1b). The phase sequences of HOB-*n*-HOB compounds (Table 1) were determined by differential scanning calorimetry (DSC, Fig. S4, ESI†) and the observation of characteristic optical textures under POM. The phase identification was confirmed by X-ray diffraction experiments. All the investigated homologues exhibited rich polymorphism of crystalline phases and, apart from the longest one, HOB-16-HOB, organize into a liquid crystalline SmC phase. However, it should be noted that the stability of the SmC phase gradually decreased with elongation of the linker, and already for the HOB-12-HOB molecule, the smectic phase became monotropic. SmC phase exhibited characteristic schlieren textures, with numerous point defects of strength ±1 (Fig. 2).

XRD patterns of the SmC phase showed a series of narrow, Bragg-type commensurate signals in the small diffraction angle range (resulting from the lamellar character of the phase and a broad wide-angle signal arising from the liquid-like positional correlations within the layers (see Fig. S3, ESI†). The smectic layer thickness for consecutive homologues was in the 4.4–5.3 nm range, which was observed to change non-linearly with the length of the spacer, showing no odd–even effect (see Fig. S5, ESI†). In contrast, an apparent odd–even effect was clearly visible at the temperatures of Iso–SmC transitions (see Fig. S6, ESI†).

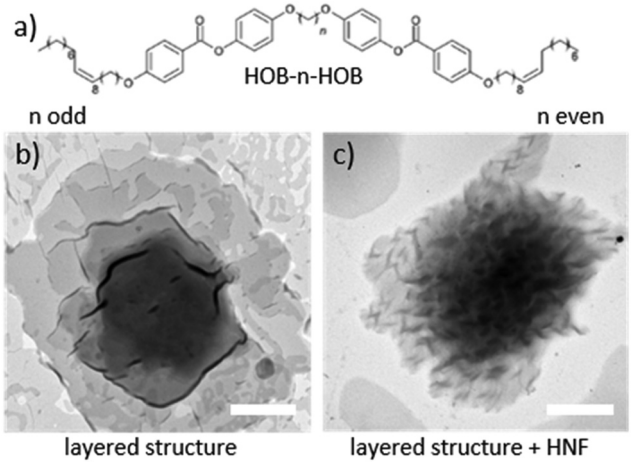

Fig. 1 Odd–even effect in HOB-*n*-HOB series. (a) Structure of HOB-*n*-HOB and shape of its most stable conformers for odd and even values of n, TEM images of (b) layered structures formed by HOB-11-HOB and (c) helical (twisted layered) structures formed by HOB-12-HOB. Scale bars represent 500 nm.

Table 1 Phase sequences of HOB-*n*-HOB dimers observed on cooling, in parentheses phase transition temperatures are given

n	Phase sequence
6	Iso (138 °C) SmC (115 °C) Cr2 (62 °C) Bx
7	Iso (106 °C) SmC (77 °C) Cr2 (67 °C) Cr1
8	Iso (124 °C) SmC (98 °C) Cr3 (91 °C) Cr2 (81 °C) Bx
9	Iso (95 °C) SmC (82 °C) Cr3 (75 °C) Cr2 (62 °C) Cr1
10	Iso (115 °C) SmC (102 °C) Cr3 (95 °C) Cr2 (74 °C) Bx
11	Iso (94 °C) SmC (86 °C) Cr2 (66 °C) Cr1
12	Iso (106 °C) SmC (100 °C) Cr2 (69 °C) Bx
16	Iso (107 °C) Cr2 (71 °C) Bx

Notation of phases: Iso, isotropic; SmC, smectic C; Cr, crystalline; Bx, dark conglomerate.

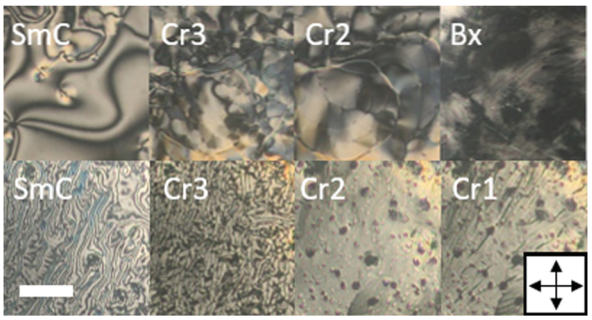

Fig. 2 POM images at temperatures corresponding to different phases of representatives of even (upper) and odd (lower) HOB-*n*-HOB. Scale bar represents 60 μm. Other XRD and POM results are shown in Fig. S2 and S3 (ESI†).

The lamellar structure was preserved in all crystalline phases, as indicated by a series of commensurate diffraction signals in their XRD patterns (see Fig. S3, ESI†). In POM observations (Fig. 2) most crystalline phases exhibited highly birefringent, non-characteristic textures. However, the clear odd–even effect was observed for the room temperature crystalline phase. Namely, in the case of even members of the HOB-*n*-HOB family, this phase showed much darker optical textures. Apparently, it had much lower birefringence, a phenomenon that may be caused by the complex mesoscale morphology of the phase, *e.g.*, the potential formation of helically twisted filaments, as suggested by TEM images.

In the next stage, HOB-*n*-HOB homologues were used to prepare composite materials with gold NPs. It has been observed that inorganic NPs strongly tend to locate in the defects of organic matrices, which can be helpful to visualise the matrix morphology *via* TEM. In our case, to ensure an efficient mixing process of gold NPs with the HOB-*n*-HOB host, we covered them with a mixed monolayer of dodecane and HOB-like ligands (see Note S1 and Fig. S7, ESI†).

Then, the obtained HOB-*n*-HOB/gold NP composites were drop casted on TEM grids, heated to 150 °C, and cooled down with a controlled rate of 3 K min^{-1} to room temperature. TEM images of the as-prepared samples (Fig. 3 and Fig. S8, ESI†) confirmed the

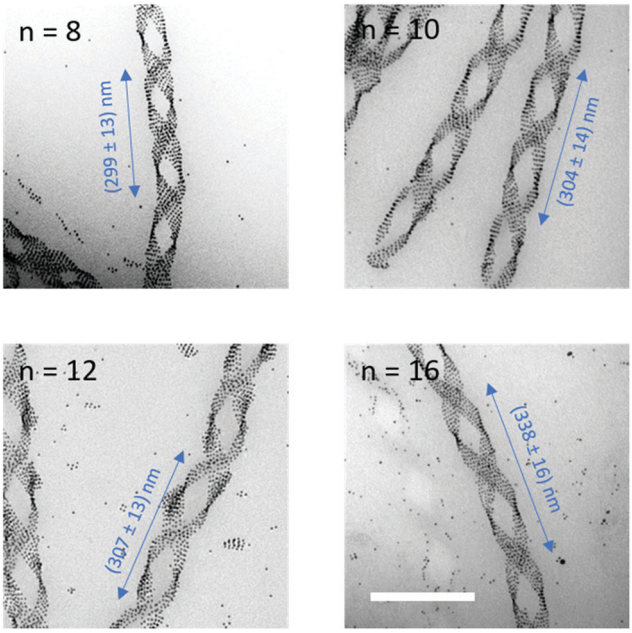

Fig. 3 Structure analysis of the helical nanocomposites prepared using even members of HOB-*n*-HOB dimers. TEM images of representative helical assemblies. Mean pitch values are indicated in the images. Scale bar represents 200 nm.

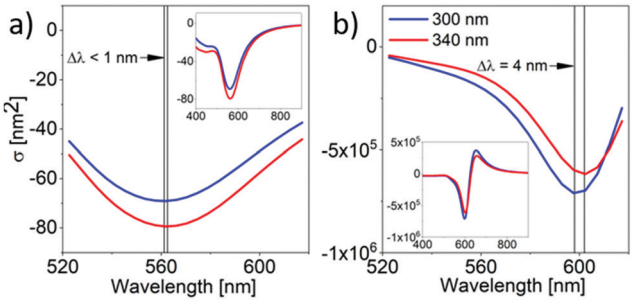

Fig. 4 Calculated PCD spectra of gold NPs with (a) 4 nm and (b) 24 nm diameter assembled on helices with pitch 300 nm (blue) and 340 nm (red). Inset shows calculated spectra in broader range of wavelength.

odd–even effect observed previously by POM for HOB-*n*-HOB compounds. Only the composites based on even HOB-*n*-HOB homologues exhibited the formation of helical structures, with Au NPs selectively deposited on their edges. Importantly, the pitch of the helical assemblies showed a clear correlation with the length of the molecular spacer, as it increased from 300 nm for $n = 8$ to 340 nm for $n = 16$. In contrast, the width of the filaments, ~70 nm, was similar for all composites. On the lowest hierarchical level, NPs form rows, with in-row distance of 6.7 nm and a length limited by the width of the organic ribbon. These linear assemblies form a periodic arrangement with an inter-row distance of 8.5 nm. On the highest level, NP clusters form twisted assemblies with periodicity determined by the curvature of helical nanofilaments. In the case of the odd-membered homologue-based composites, TEM images revealed aggregates with randomly distributed gold NPs.

Overall, these results show that even HOB-*n*-HOB compounds could be used to form nanocomposites with potentially chiral properties at the microscopic scale of single domains or the macroscopic level if assuring that the experimental conditions allow for the control of helix handedness. Moreover, helical assemblies of NPs might be interesting for chiral plasmonic applications due to their hierarchical structure and tuneable pitch. For these reasons, we decided to use computational simulations based on the T-matrix method[12] and applied to double helices made of equally-spaced NPs as models to further investigate the PCD properties of NP helical assemblies. Thus, the characterised dimensions of the helical filaments of HOB-8-HOB and HOB-16-HOB compounds were used to build our models: double helices of 4 and 24 nm diameter spherical NPs (*i.e.*, compatible with HOB-*n*-HOB matrices).[13] The modelled helices were embedded in a uniform medium with a refractive index of 1.5. Orthogonal illumination to mimic the transmission mode of CD measurements for helices growing parallel to the substrate. The results of these computational experiments revealed a clear PCD response of the distinct modelled NP helices in the wavelength range 500–700 nm (Fig. 4). The λ_{max} of PCD bands for double helices made of 24 nm diameter NPs with pitch 300 and 340 nm was 598 nm and 602 nm, respectively. Since the interparticle spacing and NP size were not varied during the experiment the observed shift could be ascribed to the change of the helical pitch that affects the nature of the plasmonic coupling. The noticed lower shift of the λ_{max} values (and overall PCD response) in the case of 4 nm diameter NPs could be explained by their weaker plasmonic properties in comparison to larger particles.

Aiming at better further understanding the behaviour of HOB-*n*-HOB compounds and their ability to form lamellar structures with helical morphologies with different pitches depending on the linker length, we carried out a series of molecular dynamics simulations experiments. Specifically, the GROMOS54a7 force field, as available within the GROMACS package,[14,15] was at first used to study the stabilisation of lamellar structures constituted by HOB-*n*-HOB mesogens with n ranging from 6 to 14 (Fig. 5 and Fig. S10–S18, ESI†) at 298 K. In the investigated stabilisation time (*ca.* 5 ns), the computational results suggest that all investigated dimeric mesogens could form stable lamellar structures, in agreement with our experimental observations (Fig. 5 and Fig. S10–S19, ESI†).

Moreover, at temperatures between 273 and 323 K, the lamellas tend to twist, which might help to explain the formation of helical filaments experimentally observed for the HOB-*n*-HOB/gold NPs composites (Fig. 5). This tendency is more significant for compounds with higher n. Finally, the distances between adjacent layers were found to increase with *n*, from 6.5 to 8 nm at 278 K (Fig. S20, ESI†), thereby helping to explain the observed increase in the helical pitch of the HOB-*n*-HOB/gold NPs composites (Fig. 3 and Fig. S10, ESI†). Unfortunately, MD simulations cannot provide information about the observed odd–even effect related to the formation of helical assemblies. However, we observed differences in the total energy of the assemblies formed by HOB-*n*-HOB with different linker lengths, which might resemble an odd–even effect.

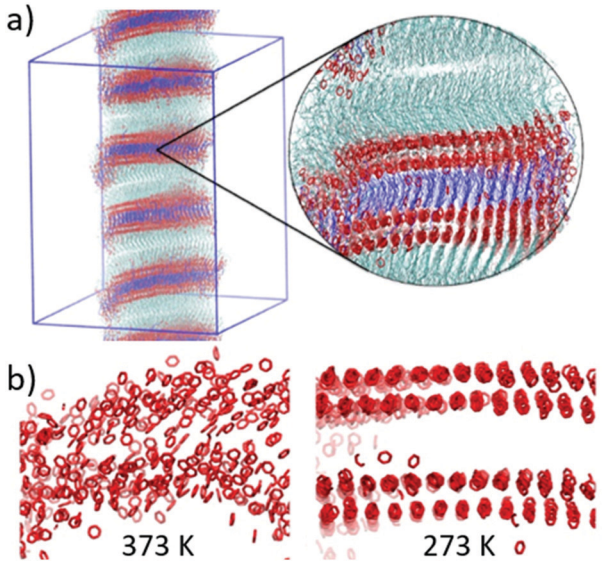

Fig. 5 (a) MD snapshot of the lamellar structure formed by the HOB-10-HOB compound. Cyan, red and blue sticks represent oleyl chains, aromatic rings, and linkers. (b) Snapshots of the MD showing the configuration adopted by the aromatic moieties in the assembled structure formed by the HOB-10-HOB at different temperatures.

For instance, the stability of the lamellar assemblies was found to be generally lower for those where n is mainly even (n = 8, 9, 10, 12 and 14) than for the assembled structures formed by mesogens with n being principally odd (6, 7, 11 and 13; Fig. S21, ESI†).

In summary, our work reveals a facile strategy for fabricating thin films of double-helical aggregates of plasmonic NPs with a tuneable helix pitch. We synthesised a series of liquid crystalline dimers with variable lengths of the alkyl spacer joining stiff aromatic arms equipped with oleyl terminal chains. Using POM and X-ray diffraction we verified that all these compounds formed lamellar crystal phases. However, only even members of the family form helical nanofilaments, which is an uncommon odd–even effect, as helical structures are typically observed in odd dimers. Large scale MD simulations of HOB-*n*-HOB assemblies confirmed the tendency to form twisted layered structures, while the differences in their total energies resemble the experimentally observed odd–even effect. TEM investigation of composites of LCs with rationally functionalised gold NPs evidence their selective deposition on the helical nanofilaments edges and the increase of the helical filaments pitch length with elongation of the alkyl linker. Implementing the experimentally derived dimensions of helical assemblies of gold NPs in modelling confirms their tuneable (determined by the pitch of the helices) chiral plasmonic character. Although the observed shift is relatively low (Note S2, ESI†), this result is a proof-of-principle example showing that modification of pitch of NP assemblies can influence the PCD response of a plasmonic composite. Thus, the strategy shown here represents an original and promising method to obtain chiral plasmonic films and the use of molecular dynamics to study morphologically chiral liquid crystals.

This research was supported by an OPUS grant from National Science Center Poland under the grant UMO-2017/27/B/ST5/02503 and Deutsche Forschungsgemeinschaft (DFG, German Research Foundation) under Germany's Excellence Strategy *via* the Excellence Cluster "3D Matter Made to Order" (No. EXC-2082/1-390761711).

Conflicts of interest

The authors declare no conflicts of interest.

Notes and references

1 Z. Hu, D. Meng, F. Lin, X. Zhu, Z. Fang and X. Wu, *Adv. Opt. Mater.*, 2019, **7**, 1801590.
2 G. Albano, G. Pescitelli and L. Di Bari, *Chem. Rev.*, 2020, **120**, 10145–10243.
3 D. P.-N. Gonçalves, M. E. Prévôt, Ş. Üstünel, T. Ogolla, A. Nemati, S. Shadpour and T. Hegmann, *Liq. Cryst. Rev.*, 2021, **9**, 1–34.
4 B. Atorf, T. Funck, T. Hegmann, S. Kempter, T. Liedl, K. Martens, H. Mühlenbernd, T. Zentgraf, B. Zhang, H. Kitzerow and M. Urbanski, *Liq. Cryst.*, 2017, **44**, 1929–1947.
5 M. Salamończyk, N. Vaupotič, D. Pociecha, R. Walker, J. M.-D. Storey, C. T. Imrie, C. Wang, C. Zhu and E. Gorecka, *Nat. Commun.*, 2019, **10**, 1922.
6 V. Borshch, Y.-K. Kim, J. Xiang, M. Gao, A. Jákli, V. P. Panov, J. K. Vij, C. T. Imrie, M. G. Tamba, G. H. Mehl and O. D. Lavrentovich, *Nat. Commun.*, 2013, **4**, 2635.
7 D. Chen, J. H. Porada, J. B. Hooper, A. Klittnick, Y. Shen, M. R. Tuchband, E. Korblova, D. Bedrov, D. M. Walba, M. A. Glaser, J. E. Maclennan and N. A. Clark, *Proc. Natl. Acad. Sci. U. S. A.*, 2013, **110**, 15931–15936.
8 M. Cestari, S. Diez-Berart, D. A. Dunmur, A. Ferrarini, M. R. de la Fuente, D. J.-B. Jackson, D. O. Lopez, G. R. Luckhurst, M. A. Perez-Jubindo, R. M. Richardson, J. Salud, B. A. Timimi and H. Zimmermann, *Phys. Rev. E: Stat., Nonlinear, Soft Matter Phys.*, 2011, **84**, 031704.
9 J. P. Abberley, R. Killah, R. Walker, J. M.-D. Storey, C. T. Imrie, M. Salamończyk, C. Zhu, E. Gorecka and D. Pociecha, *Nat. Commun.*, 2018, **9**, 228.
10 W. Lewandowski, N. Vaupotič, D. Pociecha, E. Górecka and L. M. Liz-Marzán, *Adv. Mater.*, 2020, **32**, 1905591.
11 M. Bagiński, M. Tupikowska, G. González-Rubio, M. Wójcik and W. Lewandowski, *Adv. Mater.*, 2020, **32**, 1904581.
12 M. I. Mishchenko, L. D. Travis and D. W. Mackowski, *J. Quant. Spectrosc. Radiat. Transfer*, 1996, **55**, 535–575.
13 P. Szustakiewicz, N. Kowalska, D. Grzelak, T. Narushima, M. Góra, M. Bagiński, D. Pociecha, H. Okamoto, L. M. Liz-Marzán and W. Lewandowski, *ACS Nano*, 2020, **14**, 12918–12928.
14 H. J.-C. Berendsen, D. van der Spoel and R. van Drunen, *Comput. Phys. Commun.*, 1995, **91**, 43–56.
15 B. Hess, C. Kutzner, D. van der Spoel and E. Lindahl, *J. Chem. Theory Comput.*, 2008, **4**, 435–447.